Bioorganic & Medicinal Chemistry Letters 27 (2017) 162–167

Contents lists available at ScienceDirect

Bioorganic & Medicinal Chemistry Letters

journal homepage: www.elsevier.com/locate/bmcl

# Identification and validation of small molecule modulators of the NusB-NusE interaction

Peter J. Cossar [a,3], Cong Ma [b,2,3], Christopher P. Gordon [a,1], Joseph I. Ambrus [a], Peter J. Lewis [b], Adam McCluskey [a,*]

[a] Chemistry, School of Environmental and Life Sciences, University of Newcastle, University Drive, Callaghan, NSW 2308, Australia
[b] Biology, Centre for Chemical Biology, School of Environmental and Life Sciences, University of Newcastle, University Drive, Callaghan, NSW 2308, Australia

ARTICLE INFO

*Article history:*
Received 24 September 2016
Revised 29 November 2016
Accepted 30 November 2016
Available online 1 December 2016

*Keywords:*
Protein-protein interaction
NusB-NusE
Antibiotic
Pharmacophore
In silico screening

ABSTRACT

Formation of highly possessive antitermination complexes is crucial for the efficient transcription of stable RNA in all bacteria. A key step in the formation of these complexes is the protein-protein interaction (PPI) between N-utilisation substances (Nus) B and E and thus this PPI offers a novel target for a new antibiotic class. A pharmacophore developed via a secondary structure epitope approach was utilised to perform an in silico screen of the mini-Maybridge library (56,000 compounds) which identified 25 hits of which five compounds were synthetically tractable leads. Here we report the synthesis of these five leads and their biological evaluation as potential inhibitors of the NusB-NusE PPI. Two chemically diverse scaffolds were identified to be low micro molar potent PPI inhibitors, with compound (4,6-bis(2′,4′,3.4 tetramethoxyphenyl))pyrimidine-2-sulphonamido-*N*-4-acetamide **1** and *N,N′*-[1,4-butanediylbis(oxy-4,1-phenylene)]bis(*N*-ethyl)urea **3** exhibiting $IC_{50}$ values of 6.1 μM and 19.8 μM, respectively. These inhibitors were also shown to be moderate inhibitors of Gram-positive *Bacillus subtilis* and Gram-negative *Escherichia coli* growth.



Antibiotic resistance has evolved against all clinically approved antibiotics.[1–5] Exacerbating this problem is the withdrawal of all major pharmaceutical companies from antibiotic research effectively severing the traditional antibiotic drug development pipeline.[6,7] Of equal concern is that the majority of new antibiotics are derivatives of existing drugs for which resistance rapidly arises or is even pre-existing.[8] Consequently, there is an urgent need to develop new antibiotic classes which are not predisposed to the development of drug resistance.[3,4,6–13]

The current arsenal of antibiotics typically target four major processes within bacteria: a) cell wall/membrane synthesis, b) translation, c) DNA replication and d) inhibition of metabolism.[1,2,14] Thus an underutilised target for antibiotic development is the critical process of transcription, with only Rifamycin and Fidaxomicin approved for limited clinical use as anti-transcription targeted drugs.[15] Transcription inhibition has the potential to offer a number of new targets for antibiotic drug development, and of particular interest are a number of critical protein-protein interactions (PPIs) which are essential for transcription regulation.[16,17]

There is a growing body of evidence suggesting that small molecule inhibitors can be used to inhibit PPIs.[18–21] These inhibitors typically target a small area generally at the centre of an interface which confers the essential binding interactions. These clusters of amino acids are termed "hot spots". The efficacy of PPI inhibition can vary from micro- to pico-molar potent.[22] We believed that this approach could be utilised to develop a new class of antibiotics which inhibit the formation of the antitermination complex. This large nucleoprotein assembly is unique to bacteria and functions to regulate the transcription of bacterial stable RNA (t- and rRNA).[23,24] An essential stage in the formation of this complex is the PPI between N-utilisation substance (Nus) B and N-utilisation substance E (NusB-NusE), which is responsible for initiation and recruitment of other Nus proteins and RNA Polymerase to form the antitermination complex.[25–27]

The NusB-NusE interface is characterised by the α1-helix of NusE which occupies a pocket of NusB (Fig. 1). This interaction is established by the amino acid residues H15, R16 and D19 of the

* Corresponding author.
*E-mail address:* Adam.McCluskey@newcastle.edu.au (A. McCluskey).
[1] Present address: Nanoscale Organization and Dynamics Group, School of Science and Health, Western Sydney University, Penrith South DC, NSW, Australia.
[2] Present address: Department of Applied Biology and Chemical Technology, The State Key Laboratory of Chirosciences, The Hong Kong Polytechnic University, Hung Hom, Kowloon, Hong Kong Special Administrative Region.
[3] These authors contributed equally to this work.

http://dx.doi.org/10.1016/j.bmcl.2016.11.091
0960-894X/

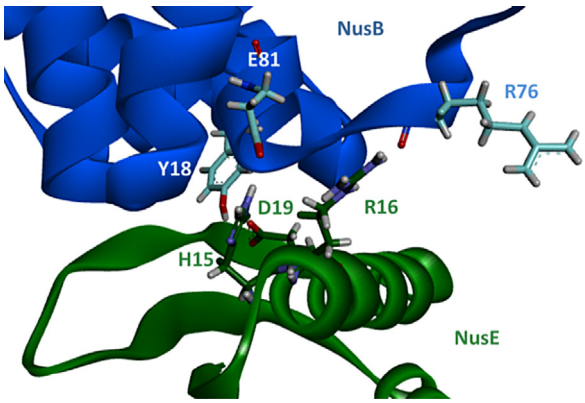


**Fig. 1.** The protein-protein interface of *Aquifex aeolicus* NusB-NusE (PDB ID 3R2C).[29] Depicted in blue is the protein NusB, with essential residues Y18, E81 and R76 highlighted (sticks). Shown in green is the α1-helix of NusE, with key amino acids H15, D19 and R16 (sticks) interacting with the binding pocket of NusB.

α1-helix forming electrostatic links with residues Y18, R76 and E81 of NusB. Combined, this pocket consists of eight hydrogen bond interactions, five of which are considered essential for heterodimer formation.[28,29]

Significantly, the residues identified above are conserved across many medically important bacterial strains including *Staphyloccus aureus*, *Streptococcus pneumoniae* and *Haemophilus influenza* (Fig. 2). Moreover, the importance of this interaction was demonstrated by two point mutations in *E. coli*, nusE100 (R72G)[30] and nusB5 (Y18D);[26] these mutations are buried in the interface and directly disrupt protein-protein binding, which in turn impedes antitermination complex formation. We hypothesised that by mimicking the α1-helix of NusE, in particular H15, R16 and D19, we could competitively inhibit the NusB-NusE PPI, and develop a platform for subsequent identification of small molecule modulators of the interaction.

To support our hypothesis that targeting the NusB-NusE PPI would prevent the assembly of this complex a 9-mer peptide, H-YDHRLLDQS-$NH_2$, was synthesised and screened as a potential inhibitor. The 9-mer returned an $IC_{50}$ of 71 ± 6.2 μM, confirming the potential to inhibit this PPI and supporting the NusB-NusE PPI interface as a potentially druggable target. Building on this we used a secondary structure epitope approach comprising a single face of the α1-helix of NusE with critical hot spot residues H15, R16 and D19 of the *A. aeolicus* NusB-NusE-*boxA* structure (PDB: 3R2C)[29] to develop a NusB-NusE interaction pharmacophore (Supplementary Data).

Our pharmacophore was developed from the partial sequence alignment of α1-helix NusE and two sequences which comprise the NusB binding pocket. Sequence alignment of NusE and NusB from *Aquifex aeolicus*, *Bacillus subtilis*, *Escherichia coli*, *Haemophilus influenza*, *Helicobacter pylori*, *Pseudomonas aeruginosa*, *Mycobacterium tuberculosis*, *Staphylococcus aureus* and *Streptococcus pneumoniae* highlighted high sequence homology and conservation across a range of bacterial species supportive of a broad spectrum antibacterial target. Of particular note, the NusE α1-helix showed minimal sequence deviation, suggesting its essential role in NusB-NusE PPI binding (Fig. 3A).

Having identified the conserved nature of these proteins, we next compared the protein alignment with published NMR and X-ray crystal structures of the NusB-NusE heterodimer in *E. coli* (PDB: 3D3B) and *A. aeolicus* (PDB: 3R2C) to determine key amino acid interactions.[28,29,31] Our analysis identified the major hydrogen bonding contributions as NusB E81 (*E. coli* E81)-NusE H15 (*E. coli* H15), NusB Y16 (*E. coli* Y18)-NusE D19 (*E. coli* D19) and NusB R76 (*E. coli* E75)-NusE R16 (*E. coli* R16). These data were consistent with the hotspot mutation identified by Friedman et al.[27] These three key amino acid interactions were then superimposed as hydrogen bond acceptor or hydrogen bond donor query features, according to the characteristics of each amino acid, over a single face of α1-helix of NusE using Discovery Studio (BIOVIA) (Fig. 2b). This gave rise to a hydrogen bond acceptor (x = 18.197; y = −30.736; z = 47.491) and two hydrogen bond donors (x = 27.296; y = −21.920; z = 42.021 and x = 25.296; y = −23.413; z = 48.000) regions. The features were used to define a central point on the residue and a location constraint sphere with a radius of 1.6 Å (based on a strong hydrogen bond interaction). In an effort to minimise potential steric clashes, a total of 21 exclusion spheres of 1.2 Å radius were installed and ultimately defined the shallow binding groove of NusB.

In total, the NusB-NusE pharmacophore comprised a hydrogen bond acceptor, two hydrogen bond donors and 21 exclusion zones.

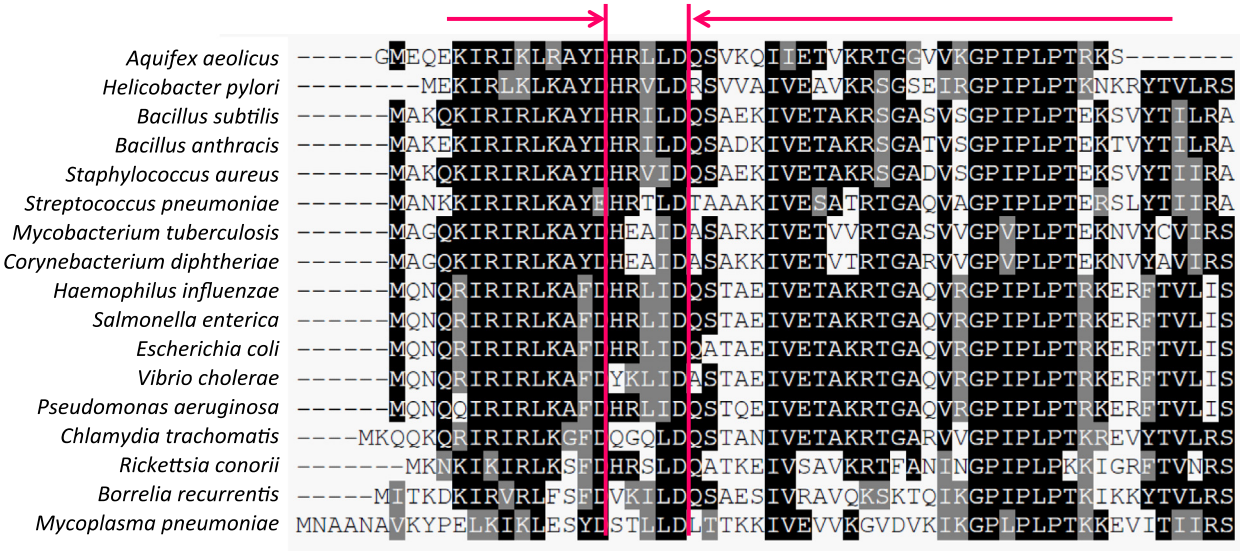


**Fig. 2.** Protein sequence alignment of NusE spanning 17 species of bacteria. Black regions indicate conserved residues; grey regions, partial conservation; white region, no residue conservation across species. The region highlighted by the red boundary represents the key NusE residues involved in binding to NusB: H15, R16 and D19.

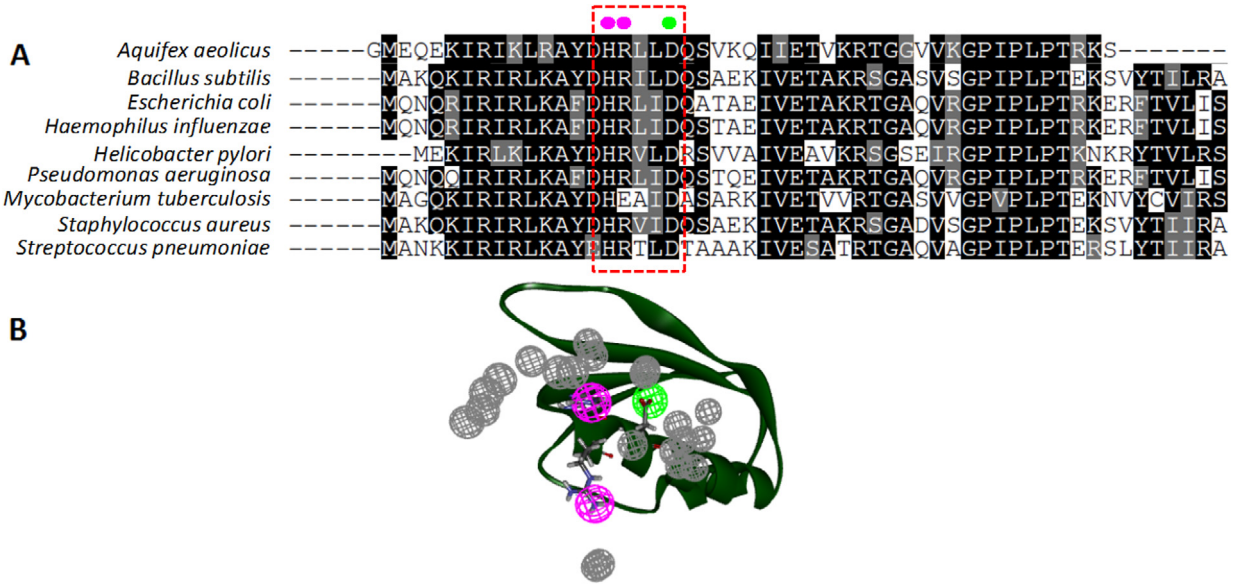


**Fig. 3.** A) The protein alignment of NusE spanning nine species of bacteria. Black regions indicate conserved residues; grey regions, partial conservation; and white regions, no residue conservation across species. The red boxed section highlights the key NusE residues involved in binding to NusB. The coloured circles above the red-boxed section denote the amino acids involved in the formation of hydrogen bond interactions where magenta = hydrogen bond donors (H15 and R16) and green = hydrogen bond acceptor (D19); B) Schematic representation of the NusB-NusE pharmacophore features overlaid onto NusE protein, where the magenta and green spheres represents hydrogen bond donors and hydrogen bond acceptors, respectively. Grey spheres represent pharmacophore exclusion zones.

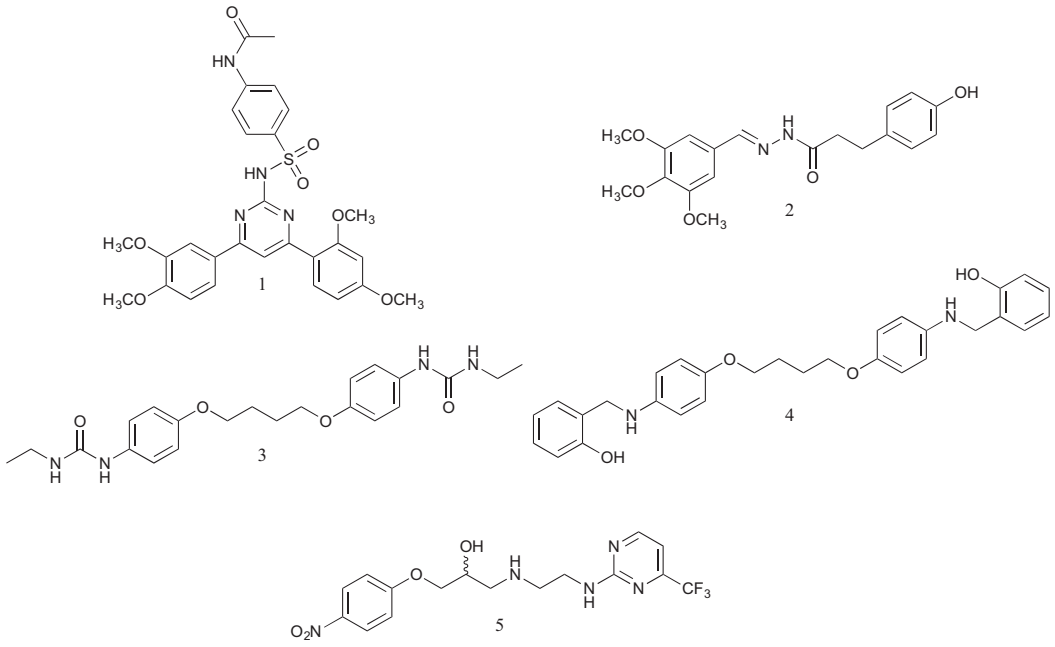


**Fig. 4.** Chemical structures of five synthetically tractable lead compounds from pharmacophore based in silico screening of the Maybridge 56,000 compound library.

Application of this pharmacophore as described by Yang et al. and an in silico screen of the mini-Maybridge 56,000 compound library identified 25 preliminary hits which were then subjected to further energy minimisations.[32] Remapping of these hits was followed by manual inspection of the resulting conformations, which as a consequence of poor pharmacophore overlap identified only five compounds, that were also deemed readily synthetically accessible (Fig. 4).[32]

To validate our pharmacophore and in silico screening hits, we set about synthesising compounds **1**–**5** for screening as NusB-NusE PPI inhibitors. Pyrimidine **1** was accessed as per Scheme 1;[33] Aldol condensation of 3,4-dimethoxyacetophenone **6**, and 2,4-dimethoxybenzaldehyde **7** gave chalcone **8** (85%). Initial efforts to cyclise **8** using literature approaches proved unsuccessful however,[33,34] with sodium isopropoxide treatment of **8** with 4-amino-*N*-(aminoiminomethylbenezenesulfonamide) resulting in a ~4:1 mixture of the desired pyrimidine **9** and the unexpected dihydropyrimidine **10**. Attempts to oxidise this mixture with Jones reagent failed to provide clean conversion to **9**. However after a number of optimisation studies pyridinium dichromate was iden-

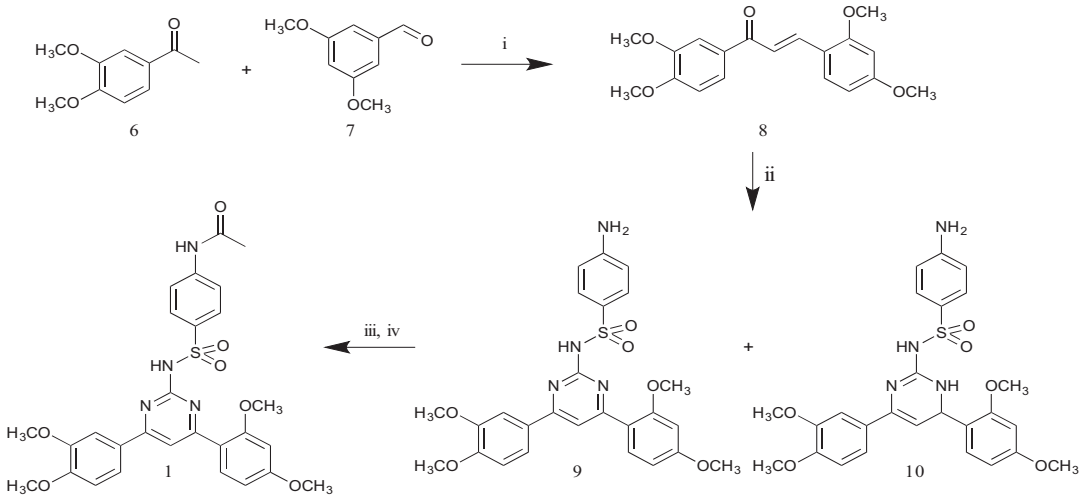

**Scheme 1.** Reagents and conditions: i) 10% NaOH(aq), EtOH, r.t., 48 h, 63%; ii) 4-amino-*N*-(aminoiminomethylbenezenesulfonamide), sodium isopropoxide, isopropanol, reflux, 16 h, (used as is without purification); iii) PDC, $CH_2Cl_2$, 16 h, 34% over 2 two-steps. iv) acetic anhydride, r.t., 50 °C, 16 h, 71%.

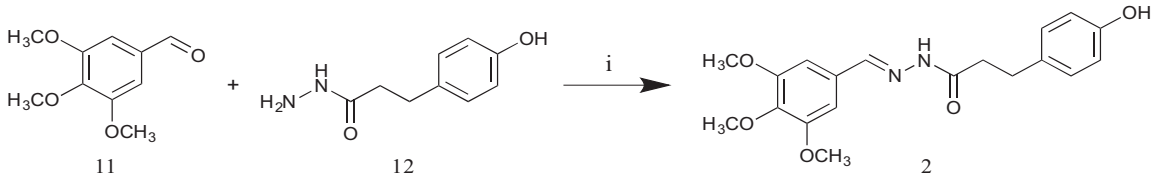

**Scheme 2.** Reagents and conditions: i) Ethanol, reflux, 16 h, 86%.

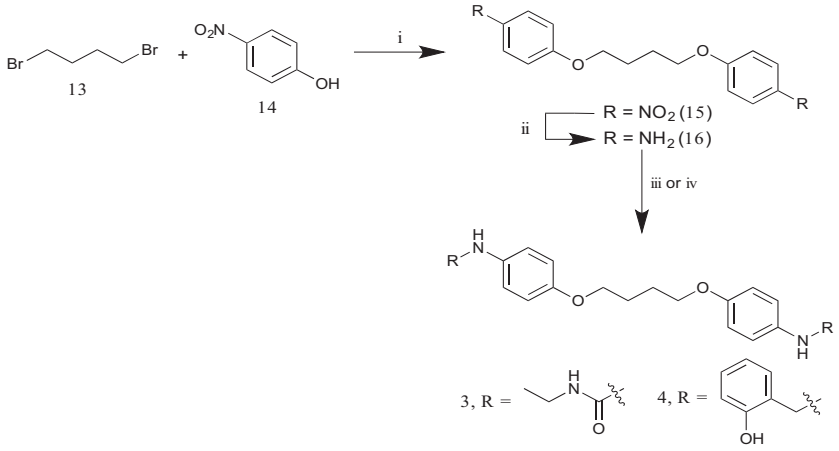

**Scheme 3.** Reagents and conditions: i) $Cs_2CO_3$, KI, $CH_3CN$, reflux, 16 h, 60%; ii) H-cube®, Raney Ni, 1,4-dioxane, 50 °C, 50 bar, 1 mL.min$^{-1}$, circulated 5 times, 99%; iii) ethyl isocyanate, THF, reflux, 16 h, 44%; iv) 2-acetoxybenzaldehyde, THF, r.t., 16 h, $NaBH_4$ 0 °C–RT, 30 min, 95%

tified as a reagent which afforded quantitative conversion of **10** to **9**. Acetic anhydride mediated acetylation of **9** gave the lead pyrimidine **1** (71%).

Hydrazide **2** was obtained in a 86% yield by condensation of 3,4,5-trimethoxybenzaldehyde **11** and 3-(4-hydroxyphenyl) propanehydrazide **12** at ethanol reflux (Scheme 2).[35]

The symmetrical ethers **3** and **4** were generated from a common intermediate **15**, produced by coupling of 1,4-dibromobutane **13** and 4-nitrophenol **14** under modified Finkelstein conditions to afford **15** (60%) (Scheme 3).[36] Optimised H-Cube flow hydrogenation conditions of 1 mL.min$^{-1}$, 50 bar $H_2$, 50 °C over Raney Ni furnished the desired diamine **16** in a quantitative yield and treatment of **16** with ethyl isocyanate gave **3** (44%). Reductive amination of **16** with 2-acetoxybenzaldehyde followed by acetate deprotection afforded **4** (98%).

Racemic **5** was accessed through a convergent approach with the epoxide **21** generated by coupling of 4-nitrophenol **14** with (±)-epichlorohydrin **19**. The key amine **20** was accessed on treatment of pyrimidine **17** with 1,2-diaminoethane **18**. Nucleophilic ring opening of epoxide **21** by **20** afforded racemic **5** (38%) (Scheme 4).[37]

With screening hits **1**–**5** in hand, their ability to inhibit the NusB-NusE PPI was examined at 25 μM compound concentration in an ELISA against *B. subtilis* NusB and NusE proteins (Table 1).[38]

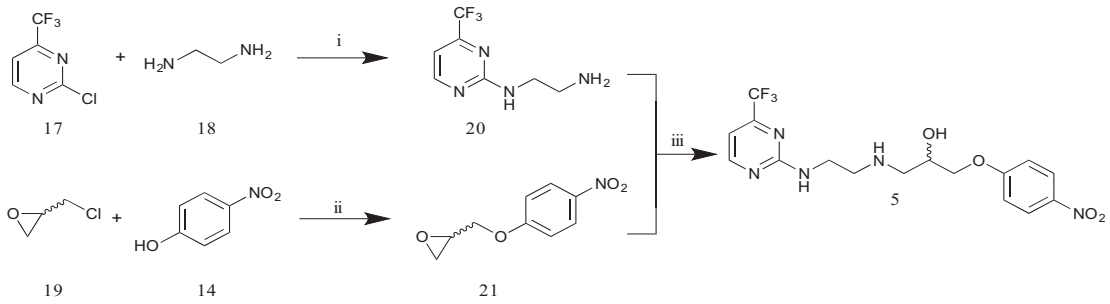


**Scheme 4.** Reagents and conditions: i) 0 °C–RT, 1 h, 76%; ii) DMF, KI, $Cs_2CO_3$, 75 °C, 3 h, 55%; iii) EtOH, reflux, overnight, 38%.

**Table 1**
The inhibition of the *B. subtilis* NusB-NusE PPI at 25 μM and the $IC_{50}$ values of analogues **1**–**5**, **8** and **9**.

| Compound | Inhibition of *nuB-nusE* interaction at 25 μM [%] | $IC_{50}$ (μM) |
|---|---|---|
| **1** | 88 | 6.1 ± 1.2 |
| **2** | 5 | n.d.[a] |
| **3** | 52 | 19.8 ± 1.7 |
| **4** | 45 | 210.0 ± 2.1 |
| **5** | n.a[b,c] | – |
| **8** | 48 | n.d. |
| **9** | 3 | n.d. |

[a] n.d. = not determined.
[b] n.a = not active.
[c] Racemate.

**Table 2**
Inhibition of *B. subtilis* and *E. coli* growth at 200 μM by analogues **1**–**5**, **8** and **9** in inhibition.

| Compound | Bacterial growth inhibition at 200 μM [%] | |
|---|---|---|
| | *Bacillus subtilis* | *Escherichia coli* |
| **1** | 9 | 21 |
| **2** | 44 | 10 |
| **3** | n.a.[a] | 17 |
| **4** | n.a. | n.a. |
| **5**[b] | 19 | 11 |

[a] n.a. = not active.
[b] Racemate.

Pleasingly compounds, **1**, **3** and **4** returned NusB-NusE PPI inhibition levels of 88%, 52% and 45% respectively with analogues **2** and **5** inactive. Full dose response evaluation of **1**, **3** and **4** against the NusB-NusE PPI returned $IC_{50}$ values of 6.1, 19.8 and 210.0 μM, respectively.

The advanced synthetic intermediates **8** and **9** were also subjected to the NusB-NusE ELISA. The high level of activity observed with **8** (48% at 25 μM) was most probably a function of the promiscuous nature of the α,β-unsaturated moiety.[39] The low levels of activity with **9**, suggests a key role for the acetate moiety in the inhibition of the NusB-NusE PPI (c.f. **1** at 88% versus **9** at 3%, at 25 μM compound concentration).

The NusB-NusE PPI targeted analogues **1**–**5** were examined for their potential inhibition of the ability to inhibit Gram positive *B. subtilis* and Gram negative *E. coli* at 200 μM compound concentration. These data are presented in Table 2.[40]

Of the five analogues evaluated only bis-ether **4** failed to elicit any degree of antibiotic response. Not surprisingly activity against Gram negative *E. coli* was uniformly low spanning 10–21% inhibition. An increased level of activity, although still modest, was observed against Gram positive *B. subtilis* with inhibition spanning 9–44%. While the observed antibiotic activity poorly correlated with the inhibition of the NusB-NusE PPI, these findings are consistent with phenotypic studies where the physicochemical properties of the molecules can have an adverse effect on cellular (here bacterial) uptake.

## Conclusions

The inhibition of the NusB-NusE interaction was demonstrated with the 9-mer, H-YDHRLLDQS-$NH_2$, 71 ± 6.2 μM potent inhibitor of this interaction. The development and subsequent screening of the Maybridge mini library with a pharmacophore based on the NusB/NusE binding interface identified five synthetically tractable hits. Synthesis of chemically diverse **1**–**5** and ELISA screening of the NusB-NusE PPI revealed three compounds (**1**, **3** and **4**) inhibited NusB-NusE binding, with >50% binding efficiency at 25 μM. Full dose response evaluation returned $IC_{50}$ values of 6.1, 19.8 and 210 μM, for **1**, **3** and **4** respectively. Subsequent screening against *B. subtilis* and *E. coli* showed moderate levels of antibacterial activity. Combined these findings validate both our pharmacophore based approach and the inhibition of the NusB-NusE PPI as a valid antibiotic drug development strategy.

Compounds **1**, **3** and **4** represent the first reported, validated, inhibitors of the NuB-NusE PPI and may allow the development of new classes of antibiotics targeting bacterial transcription.

## Acknowledgements

This work was supported by: the Australian Cancer Research Foundation, Ramaciotti Foundation, the Australian Research Council, National Health and Medical Research Council (Australia), and the University of Newcastle Early Career Research Grant (CM). CPG is the recipient of an ARC DECRA fellowship. PJC acknowledges the receipt of a University of Newcastle Postgraduate Research Scholarship. The authors thank Mohammed K. Abdel-Hamid for helpful discussions.

## A. Supplementary data

Supplementary data (pharmacophore details, NMR, IR, mass spectra and HPLC chromatograms) associated with this article can be found, in the online version, at http://dx.doi.org/10.1016/j.bmcl.2016.11.091.

## References

1. Andersson DI, Hughes D. *Nat Rev Microbiol*. 2010;8:260–271.
2. Chait R, Palmer AC, Yelin I, Kishony R. *Nat Commun*. 2016;7:10333–10341.
3. Gordon CP, Williams P, Chan WC. *J Med Chem*. 2013;56:1389–1404.
4. Brown ED, Wright GD. *Nature*. 2016;529:336–343.
5. Liu YY, Wang Y, Walsh TR, et al. *Lancet Infect Dis*. 2016;16:161–168.
6. Cooper MA, Shlaes D. *Nature*. 2011;472:32.

7. Butler MS, Cooper MA. *J Antibiot (Tokyo)*. 2011;64:413–425.
8. Mielczarek M, Devakaram RV, Ma C, et al. *Org Biomol Chem*. 2014;12:2882–2894.
9. Ma C, Yang X, Kandemir H, et al. *ACS Chem Biol*. 2013;8:1972–1980.
10. Bush K, Courvalin P, Dantas G, et al. *Nat Rev Microbiol*. 2011;9:894–896.
11. Rice LB. *Infect Control Hosp Epidemiol*. 2010;31(Suppl. 1):S7–S10.
12. Boucher HW, Talbot GH, Bradley JS, et al. *Clin Infect Dis*. 2009;48:1–12.
13. Gilbert DN, Guidos R, Boucher HW, et al. *Clin Infect Dis*. 2010;50:1081–1083.
14. O'Connell KMG, Hodgkinson JT, Sore HF, Welch M, Salmond GPC, Spring DR. *Angew Chem Int Ed Engl*. 2013;10706–10733.
15. Elgaher WAM, Fruth M, Groh M, Haupenthal J, Hartmann RW. *RSC Adv*. 2014;4:2177–2194.
16. Ma C, Yang X, Lewis PJ. *ACS Infect Dis*. 2016;2:39–46.
17. Ma C, Yang X, Lewis PJ. *Microbiol Mol Biol Rev*. 2016;80:139–160.
18. Arkin MR, Tang Y, Wells JA. *Chem Biol*. 2014;21:1102–1114.
19. Bogan AA, Thorn KS. *J Mol Biol*. 1998;280:1–9.
20. Russell RB, Alber F, Aloy P, et al. *Curr Opin Struct Biol*. 2004;14:313–324.
21. Kobe B, Guncar G, Buchholz R, et al. *Biochem Soc Trans*. 2008;36:1438–1441.
22. Chen J, Sawyer N, Regan L. *Protein Sci*. 2013;22:510–515.
23. Jin DJ, Cagliero C, Zhou YN. *FEMS Microbiol Rev*. 2012;36:269–287.
24. Robinson A, Brzoska AJ, Turner KM, et al. *Microbiol Mol Biol Rev*. 2010;74:273–297.
25. Santangelo TJ, Artsimovitch I. *Nat Rev Microbiol*. 2011;9:319–329.
26. Court DL, Patterson TA, Baker T, Costantino N, Mao X, Friedman DI. *J Bacteriol*. 1995;177:2589–2591.
27. Friedman DI, Baumann M, Baron LS. *Virology*. 1976;73:119–127.
28. Luo X, Hsiao H, Bubunenko M, et al. *Mol Cell*. 2008;32:791–802.
29. Stagno JR, Altieri AS, Bubunenko M, et al. *Nucleic Acids Res*. 2011;39:7803–7815.
30. Robledo R, Atkinson BLL, Gottesman MEE. *J Mol Biol*. 1991;220:613–619.
31. Das R, Loss S, Li J, et al. *J Mol Biol*. 2008;376:705–720.
32. Yang X, Ma C, Lewis PJ. *Methods*. 2015;86:45–50.
33. Usifoh C, Olugbade T, Onawumi G, Oluwadiya J. *J Heterocycl Chem*. 1989;26:1069–1071. *(4,6-Bis(2′,4′,3.4 tetramethoxyphenyl))pyrimidine-2-sulphonamido-N-4-acetamide* (**1**): A solution of 4-amino-*N*-(4-(2,4-dimethoxyphenyl)-6-(3,4-dimethoxyphenyl)pyrimidin-2-yl)benzenesulfonamide **9** (0.082 g, 0.157 mmol) in freshly distilled acetic anhydride (40 mL) was stirred at 50 °C for 16 h. The reaction mixture was then cooled to room temperature and saturated $NaHCO_3$ (40 mL) added dropwise followed by sonication for 30 min. The resulting suspension was then filtered and washed with water (50 mL). The precipitate was recrystallised from chloroform with drop wise addition of ethyl acetate, to afford a yellow solid (0.058 g, 71%). 214–216 °C. $^1$H NMR (400 MHz, DMSO-$d_6$) $\delta$ 11.56 (br s, 1H), 10.27 (s, 1H), 7.94 (d, $J$ = 8.7 Hz, 2H), 7.79 (d, $J$ = 9.3 Hz, 1H), 7.71 (d, $J$ = 8.8 Hz, 2H), 7.64–7.62 (m, 2H), 7.10 (d, $J$ = 8.6 Hz, 1H), 6.71–6.68 (m, 2H), 3.89–3.84 (m, 12 H), 2.04 (s, 3H). $^{13}$C NMR (151 MHz, DMSO-$d_6$) $\delta$ 172.0, 169.0, 163.6, 162.7, 159.4, 157.1, 151.4, 148.9, 143.0, 134.6, 131.8, 128.8, 128.5, 120.3, 118.2, 117.7, 111.7, 110.0 (2C), 105.9, 98.7, 55.9, 55.6, 55.6, 55.5, 24.1; LCMS (APCI$^+$) $m/z$: 565 (M+H, 100%); HRMS (ESI) calcd for $C_{28}H_{28}N_4O_7S$ (M+H) 565.1751, found 565.1747.
34. Wasfy AAF, Aly AA. *Folia Microbiol*. 2003;48:51–55.
35. McCluskey A, Daniel JA, Hadzic G, et al. *Traffic*. 2013;14:1272–1289. *(E)-3-(4-hydroxyphenyl)-N′-(3,4,5-trimethoxybenzylidene)propanehydrazide* (**2**): A solution of 3,4,5-trimethoxybenzaldehyde **11** (0.06 g, 0.31 mmol) and 3-(4-hydroxyphenyl)propane hydrazide (**12**) (0.06 g, 0.31 mmol) in ethanol (5 mL) was heated at 60 °C 18 h. The resulting reaction mixture was then adsorbed to silica and subject to column flash silica chromatography (4.2% $CH_3OH$, in $CH_2Cl_2$) to afford a white solid (0.097 g, 86%); mp 211–213 °C. $^1$H NMR (400 MHz, $CD_3OD$) $\delta$ 7.93 (s, 1H), 7.16–7.01 (m, 4H), 6.96 (s, 1H), 6.70 (d, $J$ = 7.9 Hz, 2H), 3.88 (s, 6H), 3.80 (s, 3H), 2.92 (t, $J$ = 6.9 Hz, 2H), 2.55 (t, $J$ = 7.5 Hz, 2H). $^{13}$C NMR (101 MHz, $CD_3OD$) $\delta$ (major rotamer) 171.9, 156.7, 154.63, 148.9, 141.0, 132.6, 131.0, 130.28, 116.2, 106.0, 61.16, 56.7, 37.8, 31.8. $^{13}$C NMR (101 MHz, $CD_3OD$) $\delta$ (minor rotamer) 177.1, 156.6, 154.68, 145.2, 140.8, 133.1, 131.39, 131.20, 116.1, 105.2, 61.18, 56.6, 36.0, 31.4. *1:0.3 ratio of major and minor rotamers. LRMS (ESI$^+$) $m/z$ 359 (M+H, 100%); HRMS (ESI) calcd for $C_{19}H_{22}N_2O_5$ (M+Na) 381.1421, found 381.1445.
36. *N,N′-[1,4-Butanediylbis(oxy-4,1-phenylene)]bis(N-ethyl)urea* (**3**): To a solution of 1,4-bis(4-aminophenol)butane **16** (0.20 g, 0.76 mmol) in THF (10 mL) was added ethyl isocyanate (0.13 mL, 1.62 mmol). The reaction mixture was then heated at reflux overnight. The resulting reaction mixture was then cooled to room temperature, filtered under vacuum and washed with $CH_2Cl_2$ (50 mL) to afford **3** as an off white solid (0.13 g, 44%); mp 220–222 °C. $^1$H NMR (400 MHz, DMSO-$d_6$) $\delta$ 8.16 (s, 2H), 7.26 (d, $J$ = 8.6 Hz, 4H), 6.80 (d, $J$ = 8.6 Hz, 4H), 5.95 (s, 2H), 3.94 (br m, 4H), 3.13–3.03 (m, 4H), 1.82 (br m, 4H), 1.03 (t, $J$ = 7.1 Hz, 6H); $^{13}$C NMR (101 MHz, DMSO-$d_6$) $\delta$ 155.3, 153.2, 133.7, 119.3, 114.5, 67.3, 33.9, 25.5, 15.5; LRMS (ESI$^+$) $m/z$ 437 (M+Na, 100%), 416 (M+H, 75%); HRMS (ESI) calcd for $C_{22}H_{30}N_4O_4$ (M+H) 415.2340, found 415.2359. *2,2′-[1,4-butanediylbis (oxy-4,1-phenyleneiminomethylene)]bis-phenol* (**4**): A solution of 1,4-bis(4-aminophenoxy)butane **16** (0.30 g, 1.1 mmol) and 2-acetoxybenzaldehyde (0.40 g, 2.42 mmol) in $CH_3OH$ (50 mL) was stirred at room temperature overnight. The reaction mixture was then concentrated under vacuum, diluted with THF (50 mL), cooled to 0 °C and sodium borohydride (0.50 g, 1.39 mmol) was added portion wise over 20 min. The reaction was monitored by TLC (diethyl ether/$R_f$: 0.48) and after 1 h full consumption of the starting material was observed. The reaction was quenched with water (50 mL). The solution was then concentrated under vacuum and diluted with $CH_2Cl_2$ (50 mL). The solution was then washed with 10% NaOH (50 mL) and water (2 × 50 mL). The organic layer was separated, dried over $Mg_2SO_4$ and concentrated *in vacuo* to afford an orange solid (0.52 g, 98%); mp 163–165 °C. $^1$H NMR (400 MHz, DMSO-$d_6$) $\delta$ 7.17 (d, $J$ = 6.5 Hz, 2H), 7.04–6.96 (m, 2H), 6.79 (d, $J$ = 7.4 Hz, 2H), 6.73–6.62 (m, 6H, H-2), 6.50 (d, $J$ = 8.9 Hz, 4H), 4.12 (s, 4H), 3.92–3.77 (m, 4H), 1.78–1.68 (m, 4H); $^{13}$C NMR (101 MHz, DMSO-$d_6$) $\delta$ 155.4, 150.4, 143.5, 128.6, 127.7, 126.5, 118.9, 115.8, 115.3, 113.7, 68.1, 42.7, 26.1; LRMS (ESI$^+$) $m/z$ 485(M+H, 90%); HRMS (ESI) calcd for $C_{30}H_{32}N_2O_4$ (M–H) 483.2289, found 483.2275.
37. *1-(4-Nitrophenoxy)-3-[{2-(4-(trifluoromethyl)-2-pyrimidinyl)}amino]-2-propanol* (**5**): A solution of **21** (0.34 g, 1.66 mmol) and **20** (0.27 g, 1.38 mmol) in ethanol (10 mL) was heated at reflux for overnight. The resulting reaction mixture was then subjected to silica gel column chromatography (1:10:89 $NH_4OH$:MeOH: $CH_2Cl_2$) to afford **5** as a white solid (0.23 g, 38%), 130–131 °C. $^1$H NMR (400 MHz, DMSO-$d_6$) $\delta$ 8.59 (br s, 1H), 8.19 (d, $J$ = 9.2 Hz, 2H), 7.78 (br d, $J$ = 26.1 Hz, 1H), 7.14 (d, $J$ = 9.3 Hz, 2H), 6.93 (d, $J$ = 4.9 Hz, 1H), 5.06 (d, $J$ = 3.9 Hz, 1H), 4.07 (ddd, $J$ = 16.2, 10.0, 5.2 Hz, 2H), 3.89 (d, $J$ = 3.9 Hz, 1H), 3.40–3.35 (m, 2H), 2.79–2.57 (m, 4H), 1.89 (br s, 1H). $^{13}$C NMR (151 MHz, $CDCl_3$) $\delta$ 163.7, 162.7, 160.6 156.6 (dd, $J$ = 36.2, 36.8 Hz), 141.9, 126.1, 120.6 (dd, $J$ = 550.4, 274.9 Hz), 114.7, 105.9 (d, $J$ = 2.3 Hz), 71.2, 68.4, 51.4, 48.9, 41.4; LRMS (ESI$^+$) $m/z$ 402 (M$^+$, 100%); HRMS (ESI) calcd for $C_{16}H_{18}F_3N_5O_4$ (M+H) 402.1384, found 402.1380.
38. *ELISA based Screening:* Purified full-length *B. subtilis* NusB was diluted to 250 nM in phosphate buffered saline (PBS) buffer and 100 μL of the solution was added into NUNC Maxisorp™ microtitre plate wells. Following overnight incubation with the NusB solution at 4 °C the wells were washed 3 times with 300 μL of PBS buffer and blocked with 300 μL of 1% (w/v) bovine serum albumin (BSA) dissolved in PBS buffer at room temperature. After blocking for 2 h, plates were washed three times with wash buffer (PBS, 0.05% (v/v) Tween-20). The appropriate inhibitor (Table 1) and 100 μL of affinity purified glutathione-S-transferase (GST) tagged NusE at 200 nM were incubated at 37 °C for 15 min then were added to each well and incubated for 1 h at room temperature. Unbound NusE was removed by washing each well 3 times in 300 μL of wash buffer. Rabbit anti-GST primary antibody (100 μL, 1:2000 in PBS) was added to each well and incubated for 1 h at room temperature. After washing, goat-anti-rabbit HRP secondary antibody (1:2000 in PBS) was added to each well and incubated for 1 h at room temperature then washed 3 times in 300 μL of wash buffer. Visualisation of PPI was achieved by addition of 100 μL TMB (3,3′,5,5′-tetramethylbenzidine liquid substrate system for ELISA, Sigma-Aldrich) to each well. The plate was incubated in a plate reader (FLUOstar Optima) at 37 °C with 200 rpm shaking for 6 min. The optical density of each well was taken at 600 nm.
39. Baell JB, Holloway GA. *J Med Chem*. 2010;53:2719–2740.
40. *Growth inhibition assay:* The compounds were dissolved to 50 mM in DMSO and serially diluted in 100 μL of Luria broth (LB) to a concentration of 200 μM in a 96-well NUNC Microwell™ plate. *E. coli* DH5α and *B. subtilis* were grown at 37 °C in 5 mL LB with shaking until the optical density reached 0.6–0.7 AU, and 5 μL of the culture was added to each well. The plate was incubated in the plate reader (FLUOstar Optima) at 37 °C with 200 rpm shaking. The optical density of the culture was taken every 10 min using LB as the blank for 16 h at 600 nm. The samples were tested in triplicate and the growth pattern of each sample was compared to cells exposed to equal amounts of DMSO.